LARGE-EDDY SIMULATIONS OF NATURE-BASED SOLUTIONS EFFECTIVENESS IN POLLUTANT REMOVAL FROM URBAN CANYONS

Silvana Di Sabatino[1], Carlo Cintolesi[1]

[1]Department of Physics and Astronomy, University of Bologna, Bologna, Italy

Abstract: The paradigmatic case of a periodic square urban canyon at $Re = 2 \times 10^4$, where a pollutant is released at the street level, represents the basic geometry to investigate the effectiveness of grey and green Nature-Based Solutions (NBSs) in enhancing pollutant dispersion. First, the simulation approach is validated successfully against laboratory and numerical datasets. Second, the NBSs are virtually introduced and analysed: the grey NBS (roof obstacles) generates highly energetic turbulence motions at the rooftop level, which destroys the sharp shear layer and increases the mixing and the pollutant dispersion. Larger vertical turbulent mass fluxes near the upwind building, where pollution accumulates, are detected. The reduction in the pollution concentration within the canyon is about 34%. The green NBS (roof trees), instead, mainly acts as a sink of momentum and as a predominant effect decreasing the forced circulation within the canyon, leading to a slightly higher pollutant concentration. In this case, the shear layer is destabilised, but the atmospheric wind is less energetic throughout the area above the canyon. This generates a reduction of turbulent mixing and vertical transport at the interface.

Key words: Nature-Based Solutions, Urban Canyon, Rooftop trees, Large-Eddy Simulations, OpenFOAM.

INTRODUCTION

Strategies for improving the pollution removal from urban canyons are of major importance when the control of air quality in cities is in question. In the last decade, increased attention has been paid to the use of Nature-Based Solutions (NBSs), and the European Commission itself has made them a crucial tool for structuring mitigation measures and adapting to the adverse effects of climate change (Faivre et al, 2017). In an idealized urban canyon, the removal occurs at the building-roof level. Overall, it is supported by turbulent kinematic fluxes and limited by roof shear, which creates a sharp separation between the recirculation region inside the canyon and the atmospheric wind above (Michioka et al., 2014).

In this work, the roof morphology is modified through the introduction of two NBSs of grey and green type, *i.e.* rectangular solid infrastructures and low trees, respectively. The effect of these NBSs on the general air dynamics is studied employing accurate numerical experiment, performed adopting the Large-Eddy Simulation (LES) approach. Such methodology realistically reproduces three-dimensional and time-dependent turbulent motions, directly resolving the more energetic scale of motion and modelling via a Sub-Grid Scale (SGS) model the less energetic ones. There are here reported some of the first high-resolution numerical studies of NBS using LES, which, due to its ability to resolve transient and three-dimensional motion, as well as its advanced turbulent modelling, is most suitable than the wider-used Reynolds-Averaged Navier-Stokes simulations when the purpose is to analysed pollutant dispersion mechanisms in urban contexts. Such methodology is increasingly used for various practical applications but is still not widely used due to its relatively higher computational cost and lower numerical robustness, which requires special attention in numerical settings and computational-grid design.

SIMULATION APPROACH

Mathematical model

The air is modelled as an incompressible gas and the pollutant concentration is a passive scalar that is realised, advected and diffused in air. If trees are present, their canopy is modelled as a moment sink S_i^{tree}. The equations of motion are:

$$\frac{\partial u_j}{\partial x_j} = 0, \qquad (1)$$

$$\frac{\partial u_i}{\partial t} + u_j \frac{\partial u_i}{\partial x_j} = -\frac{\partial p}{\partial x_i} + \nu \frac{\partial^2 u_i}{\partial x_j \partial x_j} - S_i^{tree}, \qquad (2)$$

$$\frac{\partial c}{\partial t} + u_j \frac{\partial c}{\partial x_j} = \lambda \frac{\partial^2 c}{\partial x_j \partial x_j}, \qquad (3)$$

where the summation on the repeated index is assumed, u_i are the velocity components, p is the pressure, ν is the kinematic viscosity, c is the pollutant concentration and λ its molecular diffusivity. The sink due to the foliage reads:

$$S_i^{tree} = C_d \cdot LAD \cdot |u| \cdot u_i \qquad (4)$$

whit C_d is the drag coefficient and LAD is the Leaf Area Density, which varies with respect to the distance from the trunk and depends on the type of tree under analysis. Linked to the latter, the Leaf Area Index is defined as the integral of the LAD function.

Numerical methodology
The equations of motion have been resolved adopting the LES technique (e.g. Rodi et al., 2013). The sub-grid scale model used is the dynamic Lagrangian model proposed by Menveau et al. (1996). Such a model is based on the classical Smagorisky (1963) model, but the empirical parameter is computed dynamically and estimated in each computational cell through a Lagrangian procedure. For this reason, the model is particularly suitable for reproducing anisotropic and localised turbulence, which characterised the system under analysis. The effects of turbulence on pollutant concentration are also reproduced taking advantage of the Reynolds analogy. Details on the sub-grid scale model used are not reported here for the sake of brevity; we refer to Cintolesi et al. (2021) for a detailed discussion.

Implementation and schemes
The mathematical model reported, as well as the dynamic Lagrangian SGS model, has been implemented in homemade software, developed within the OpenFOAM (2018) toolbox. The discretization schemes ensure a global accuracy of the second order.

CASE STUDIES

The cases under investigation are based on the same idealised geometry: the reference case is a periodic array of infinite square urban canyons (Figure 1, left panel) of height H. The obstacle case is obtained by adding to the rooftop a series of rectangular blocks (Figure 1, centre panel) of height $0.1H$, depth and width $0.05H$, placed at a distance of $0.15H$ from each other. The tree case, instead, has a series of low-growing trees on the rooftop: they are composed by a solid cylindric trunk (diameter $0.02H$ and height $0.15H$) placed at a distance $0.1H$ from the edge and $0.4H$ from each other. The canopy is a porous medium with a sphere shape, centred at the end of the trunk. Two radii were chosen to represent small trees (radius $0.05H$) and big trees (radius $0.1H$). Such dimensions were selected to be representative of Laurel trees, with a $C_d = 0.2$ and a Leaf Area Index of 8, while the LAD has been chosen to be higher in the external par and lower near the trunk. It can be observed that the settings of the size and distribution of the elements on the roof are somewhat subjective; this contribution is one of the first work on this topic and a sensitivity study on the parameters used has not been conducted yet.
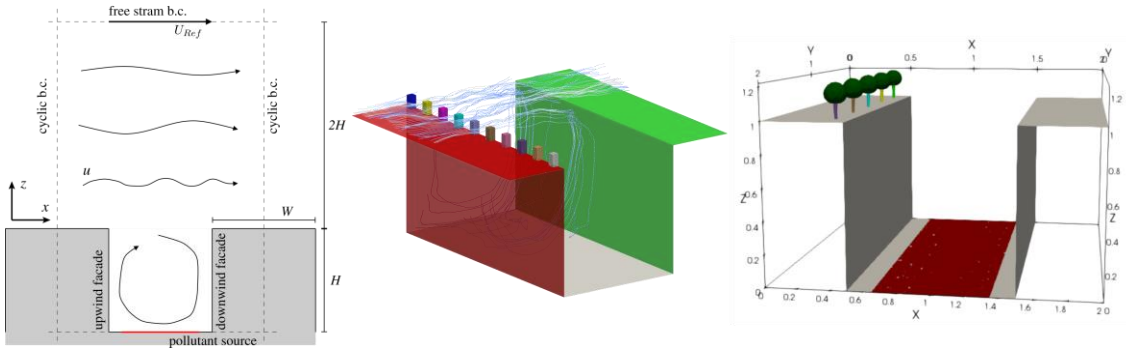
Figure 1: Sketch of case studies. Left, reference case: urban canyon with smooth roof. Centre, obstacle case: canyon with grey infrastructure on the roof. Right, tree case: canyon with trees on the roof.

In all cases, the atmospheric wind is perpendicular to the canyon axis, and the Reynolds number based on the free-stream velocity is $Re = 2 \times 10^4$ (hence, in regime of Reynolds independence). The pollutant is realised with constant flux at the street level from a band of width $0.7H$, mimicking the traffic pollution from a roadway.

Computational mesh and validation

The three geometries are discretized by 1 592 562 cells, 4 087 700 cells, and 2 040 786 cells for the reference, obstacle and tree cases (respectively). The computational grid is refined near the solid surfaces ensuring the direct resolution of the wall-boundary layer, and a refinement region is created near the obstacles where turbulence is expected to be more intense. Simulations have been run till the systems reach a statistically steady state before the statistics have been computed. The simulations approach has been successfully validated by comparing the results obtained in the reference case with experimental and numerical datasets reported in the literature (see Cintolesi et al., 2021).

OBSTACLE-ROOF CASE

In this case solid infrastructure have been added to destabilise the sharp shear layer that establishes at the roof level ($z/H = 1$) and that separates the in-canyon circulation to the surrounding atmospheric flow. Figure 2 shows the velocity streamlines within the canyon for the reference and the obstacle case. The general circulation is not altered but the presence of the obstacles weakens and reduces the extent of the recirculation zones at the upwind façade ($x/H = 0.5$). This is significant for the enhancement of pollutant dispersion, as the highest concentrations are found on the upwind façade where the pollutant is transported by the principal canyon vortex. In particular, the reduction of recirculation at roof level allows a higher momentum mass exchange with the atmosphere. It can be noted also that the separation line between the internal vortex and the atmospheric flow is slightly curved upwards.
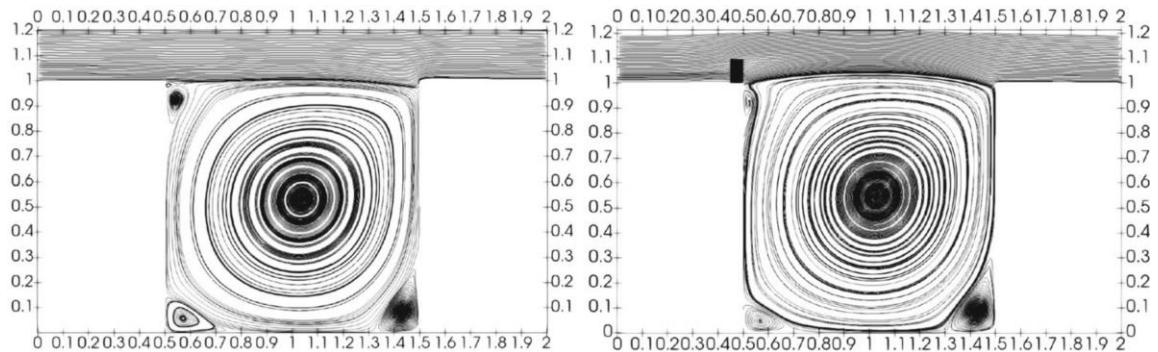

Figure 2: Streamlines of the reference case (left panel) and obstacle case (right panel).

The turbulent kinetic energy ($u_i'u_i'/2$) and the turbulent momentum kinetic fluxes ($u'w'$) - not shown – exhibits higher values at the interface when obstacles are present, along with a pick that is slightly shifted

upward. Thus, the obstacles act as turbulent generators, increasing the level of turbulence at the interface between the canyon and the atmosphere, and weakening the flow separation. The interface is less stable and turbulent mixing and transport of mass and momentum in the vertical direction are intensified.
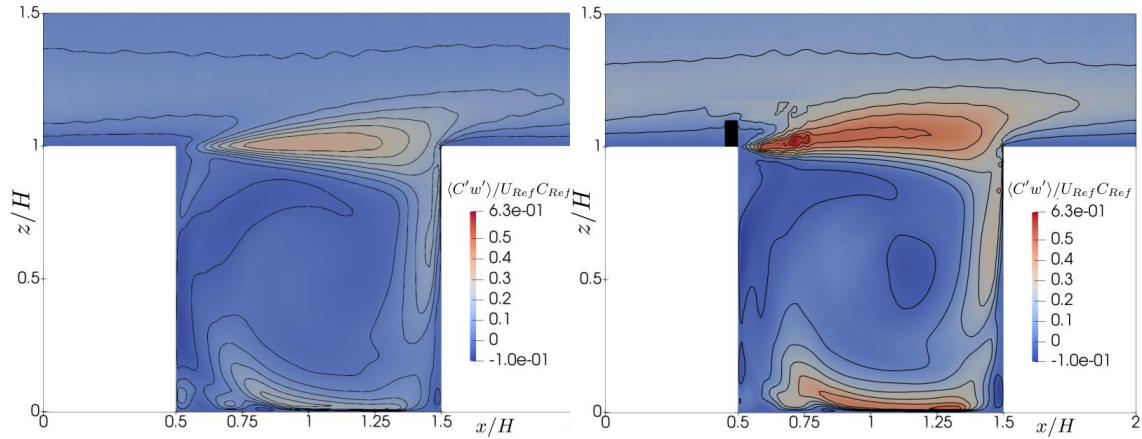

Figure 3: Dimensionless turbulent concentration fluxes in the reference (left) and obstacle case (right).

Figure 3 reports the dimensionless turbulent concentration fluxes ($c'w'$). Two main spots of high value are detectable: above the street where the pollutant is realised, and at the canyon-atmosphere interface. The turbulence generated by obstacles destabilised the roof shear layer and induce a more efficient vertical mixing at the interface. To better quantify the effectiveness of obstacles in enhancing the pollution transfer through the roof interface, the convective transfer coefficient (Barlow and Belcher, 2002) was computed as the integral along the interface of the vertical concentration fluxes $cw >$, and it is 7% higher (per unit of time) in the obstacle case. Also, a direct estimation of the concentration of pollutant in the canyon reveals that the obstacle case has 34% lower concentration that the reference case with smooth roof.

TREE-ROOF CASES

The tree-roof case wants to assess whether green infrastructure can help the dispersion of pollutants in urban canyons. The velocity streamlines do not differ substantially from the reference case; hence, the discussion is supported by plotting key quantities over vertical lines placed at three selected locations: near the upwind façade ($x/H = 0.75$), in the canyon centre ($x/H = 1$), near the downwind façade ($x/H = 1.25$). Figure 4 shows the dimensionless streamwise velocity (u) and the turbulent kinetic momentum fluxes ($u'w'$) along such three vertical lines. Overall, the velocity field is not substantially altered by the presence of trees within the canyon, and a decrease in velocity is detectable only at the canopy level (marked with a dotted line) as a result of the leaf-induced momentum sink. Interestingly, the velocity reduction produced is weakly correlated with canopy size, and both large and small trees produce similar profiles. Regarding turbulent fluxes, no relevant differences can be observed within the canyon, while lower peaks at the interface and the generation of a secondary peaks localised at the height of the trees can be detected. For the secondary peaks, trees with a larger crown produce more intense turbulent flows.
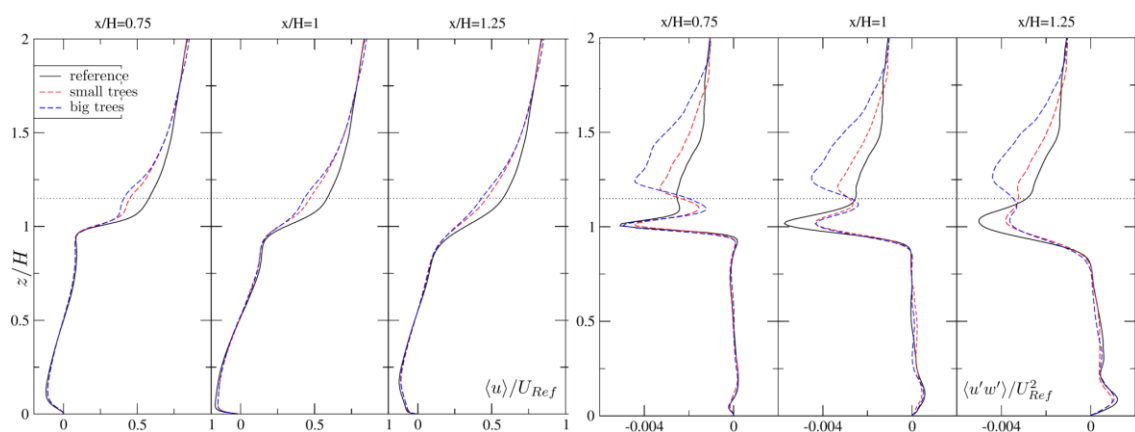
Figure 4: Dimensionless streamwise velocity (left panel) and turbulent kinetic momentum fluxes (right panel) along three selected vertical lines within the canyon.

An analysis of pollutant concentration fluxes and the average concentration – not reported - within the canyon reveals that this configuration of trees tend to slightly decrease the pollutant dispersion, and higher concentration are detected in the canyon compared to the reference case. This can be due also to the reduction of turbulence intensity highlighted at the interface ($z/H = 1$).

FINAL REMARKS

In the present study has been shown that grey infrastructures (solid obstacles) on rooftop have positive effects on the dispersion of pollutants from an urban canyon, mainly due to the turbulence generated at the canyon-atmosphere interface with enhances turbulent mixing and transport. Instead, green infrastructures (trees) are not as effective for the same purpose and even show a slightly adverse effect. This is probably due to the fact that tree canopies act by reducing atmospheric wind speed and are less effective in generating turbulence than solid obstacles. Furthermore, obstacles act at roof level by destabilising the shear layer and, thus, the interface separating the internal circulation of the canyon from atmospheric wind; whereas trees act at the canopy level, which is positioned higher up. The trees are therefore less effective in weakening the separation between in- and out-canyon flows. A different configuration of the trees, as well as the introduction of a pollutant-sink term due to canopy trees, could lead to better results in terms reduction of canyon pollution and will be the subject of future studies.

REFERENCES

Barlow J., S. Belcher, 2002: A wind tunnel model for quantifying fluxes in the urban boundary layer. *Boundary-Layer Meteorol* **104**.

Cintolesi C., B. Pulvirenti, S. Di Sabatino, 2021: Large-Eddy Simulations of Pollutant Removal Enhancement from Urban Canyons. *Boundary-Layer Meteorol.*, **180**, 79-104.

Faivre N., M. Fritz, T. Freitas, B. De Boissezon and S. Vandewoestijne, 2017: Nature-Based Solutions in the EU: Innovating with nature to address social, economic and environmental challenges. *Environmental Research*, **159**.

Michioka T., A. Sato, H. Takimoto, M. Kanda, 2011: Large-eddy simulation for the mechanism of pollutant removal from a two-dimensional street canyon. *Boundary-Layer Meteorol,* **138.**

Meneveau C., T. Lund, W. Cabot, 1996: A Lagrangian dynamic subgrid-scale model of turbulence. *J. Fluid Mech.,* 316-353.

OpenFOAM, 2018: The OpenFOAM Foundation, version 6.0. Available online: openfoam.org (accessed on 1 May 2019).

Rodi W., G. Constantinescu, T. Stoesser, 2013: Large-eddy simulation in hydraulics, 3rd edn. CRC Press, Taylor and Francis Group, Boca Raton.

Smagorinsky, J., 1963: General circulation experiments with the primitive equations: I: the basic experiment. *Mon Weather Rev,* 91-99